Star Formation in NGC 6611 with ADONIS and Hubble

D. CURRIE, K. KISSELL, ED SHAYA, P. AVIZONIS AND D. DOWLING, University of Maryland
D. BONACCINI, ESO

New details of the star-formation process have been revealed by a co-ordinated use of the ADONIS system on the 3.6-metre telescope at La Silla, in combination with data from the WFPC2 Camera of the Hubble Space Telescope. In this very preliminary report, we illustrate some of the unique capabilities of the ADONIS system for high-resolution near-infrared observations of the stellar formation process.

The observations address NGC 6611 (also known as M16 or as the Eagle Nebula). This is a dense molecular cloud in which a small cluster of high-mass stars has recently formed. The very high ultraviolet flux emitted by these early-type stars has dispersed or "photo-eroded" surrounding regions of the molecular cloud. Variations in the density of the gas and dust of the cloud have resulted in an uneven irregular erosion, forming the "elephant trunks" seen in the ground-based image shown in Figure 1. Investigation of the details of the resulting structure gives a measure of the resistance of the cloud to the photo-erosion process, which, in turn, is a measure of the density of the various regions of the cloud. While other properties, such as the magnetic field and local temperature, may also affect the rate of erosion, this may be one of the most direct methods of measuring the density profile about pre-protostellar objects.

These data were taken by Douglas Currie with Kenneth Kissell of the University of Maryland and Domenico Bonaccini of ESO. The generous support of the La Silla 3.6-m telescope team was also determinant. This preliminary image processing has been conducted by Ed Shaya, Petras Avizonis, and Dan Dowling of the University of Maryland. The analysis of these data will be conducted by this group, in collaboration with other members on the WPFC2 IDT team (i.e., Jeff Hester, Paul Scowen and others) and other individuals at the University of Maryland. The observations described here were conducted in early May, 1996 on the 3.6-metre telescope at La Silla using the ADONIS adaptive optics system and the SHARP II NICMOS Camera.

The scientific objectives of these observations are to provide observational data for the understanding of star-formation processes. These three areas of particular interest to us and the targets of our succeeding analyses consist of:

Figure 1: M16 Nebula (North to the top). A ground-based image of the nebula obtained by David Malin illustrates the context of our observations of M16. Observationally, M16 consists of a cluster of early-type, very luminous, very massive young stars and an HII region containing "elephant trunks" or "columns". The early-type stars have photo-eroded most of the molecular cloud leaving behind the structures in the HII region. Fluctuations in density in the original molecular cloud caused irregularities in the photo-erosion process. In particular, on the large scale, the "elephant trunks" pointing north-west, i.e., towards the hot stars, are the result of large-scale density fluctuations which have shielded portions of the molecular cloud from photo-erosion. On the smaller scale, which is our area of interest, we will see "bumps" and "pimples" caused by the smaller density variations. We believe that this is due to the excess material in self-gravitating pre-protostellar regions. The solid outline indicates the extent of the WFPC2 image.

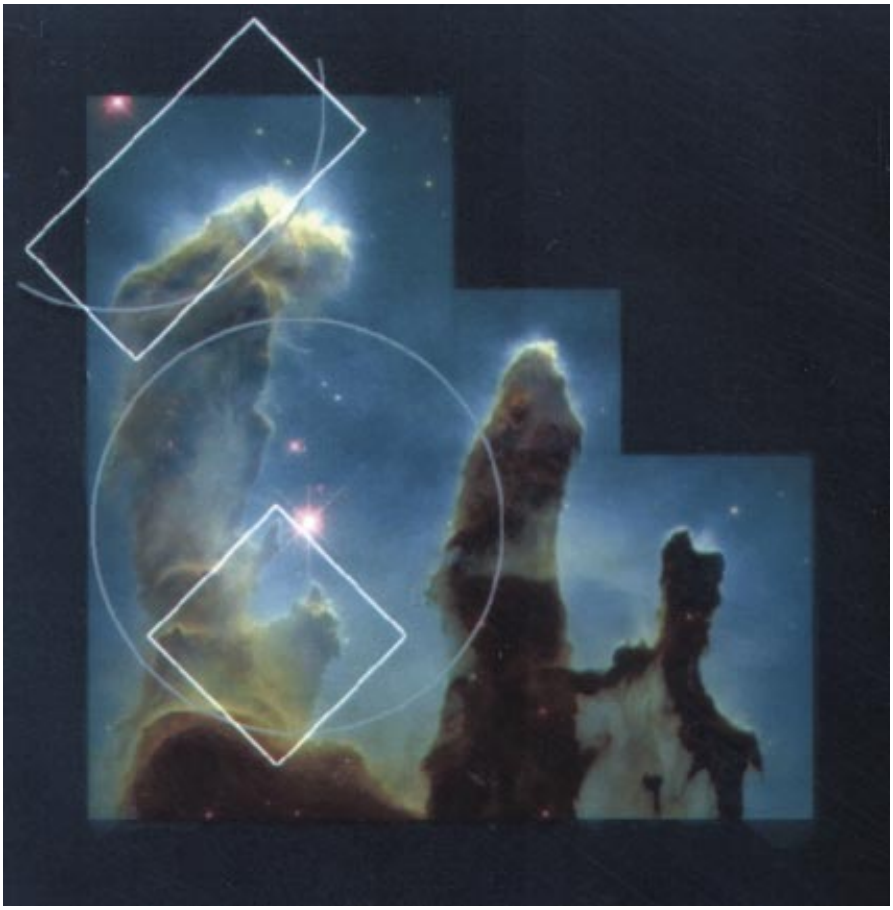

Figure 2: WFPC2 emission-line image of the central portion of the HII region of M16. North is on the upper left. This was obtained on the WFPC2 of the Hubble Space Telescope on 22 April 1995 (Hester et al., 1996) and is a colour composite in which the red image is in the ionised sulphur [SII] filter, the green image is Hα and the blue image is doubly ionised oxygen [OIII]. This colour sequence is in order of the energy of ionisation. The solid outlines illustrate the boundary of the regions mapped using the ADONIS System on the 3.6-metre telescope at La Silla. The upper region (denoted the "TIP") explores the top of Column III and the region above the column. The lower region, denoted "367", is located near Walker Star #367. The gray circles indicate the outer limits of the ADONIS field of view due to the optical mount for a beam splitter in the ADONIS optical system.

developed initially by Walker, et al. (1988), by Chini et al. (1990), and by Hillenbrand et al. (1993). In each case, the primary limitations have been resolution (with overlap of objects due to the extreme crowding), and limiting magnitude in various bands. The combination of the increased resolution and the deeper exposures of the ADONIS data, and the capabilities of Hubble, should permit a significant extension of the analysis of Hillenbrand.

(1) Density Profiles of Dust and Gas as a Function of the Stage of Stellar Formation

The dimensions of the features revealed in the Hubble data yield information related to the density profile of the in-falling dust and gas. For example, we can obtain a "characteristic size" related to the current stage of the formation process for a given object. The ESO data should allow us to place an object within the normal classification schemes for star formation, i.e., from the classes described by Hillenbrand to the very early class described, for example, by André (1995).

(2) Direct Evidence of Pre-Main Sequence Objects for the Fainter Components of M16

M16 has long been an interesting region in the search for "pre-main sequence" objects. Such work has been

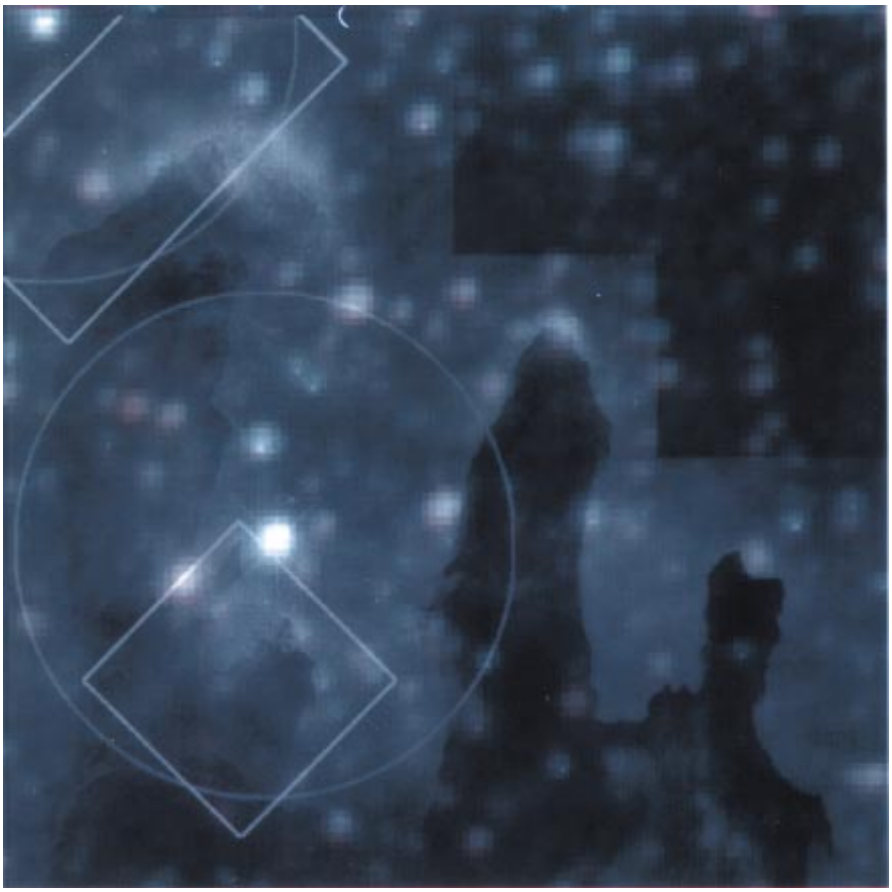

Figure 3: Infrared Structure of the WFPC2 area. North is on the upper left. This figure illustrates the general context of the Hubble Space Telescope observations, as illustrated by recent ground-based observations in H and K bands (Hillenbrand et al., 1993). The published version of the Hillenbrand data covers 225 square minutes to a limiting magnitude of about 14. Figure 2 shows only the portion which directly corresponds to our Hubble image. This image is a colour composite using the J and K magnitudes as the blue and red images. The white "ghost" image is the same region in the filter for Hα emission from our WFPC2 observations. Thus the white "cores" of the stars come from the Hubble data. The regions which were observed at La Silla in J, H, and K bands are indicated by the rectangular outlines.

Adaptive Optics at ESO is Delivering Exciting Science

Adonis is the ADaptive Optics Near Infrared System that ESO is regularly offering since December 1994 on the La Silla 3.6-m telescope. The instrument has been built by the Observatoire de Paris-Meudon as a follow-up of the previous ComeOn+ system. It is equipped with Sharp II and Comic IR cameras, to cover the range 1–5 μm. They have respectively been built by the Max-Planck-Institut für Extraterrestrische Physik in Garching and a team from Observatoire de Meudon and Observatoire de Grenoble in France. Foreoptics allows for polarimetry, Fabry-Perot Spectroscopic imaging with resolving powers R = 900 and 2500 in K-band, and by the time you will read this article also coronography. For a detailed description see our web pages on www.eso.org.

Observations with Adaptive Optics is still a virgin territory in astronomy, with plenty of fruits to pick. Many observers have already used it and an updated publication list is kept in the Web. Adonis is so far regularly oversubscribed by more than a factor 2. We often see excited scientists leaving La Silla with their data, and we encourage them to publish in The Messenger *reports on their preliminary results. This will help new observers and encourage healthy competition.*

Figure 1: Adonis K-band 10-sec-exposure image of a point source obtained at the 3.6-m telescope on La Silla (top). The look-up table is power 1/4th in order to highlight the low level features. The corresponding uncorrected 10-sec-exposure image is shown at the bottom.

If you are planning to observe with Adaptive Optics for the first time, some preparation to find the best tricks to observe your own object is necessary. Especially the data calibration, both spatial and photometric, requires good planning of the observing nights. ESO is trying to help with web pages at the www.eso.org site, which will act more and more as user manual and tips recorder on line, as well as with technical support during your proposal preparation.

For the data processing, ESO has come up with a dedicated software package called Eclipse, which has a pipeline, number crunching approach. The goal is that the observer checks his/her data possibly during the observing run itself, in order to better focus on the scientific targets he/she is getting. Thanks to a collaboration with Dr. J. Christou from the Starfire Optical Range [NM-USA], we will attach to Eclipse powerful iterative deconvolution software tailored to adaptive optics data.

Domenico Bonaccini,
dbonacci@eso.org

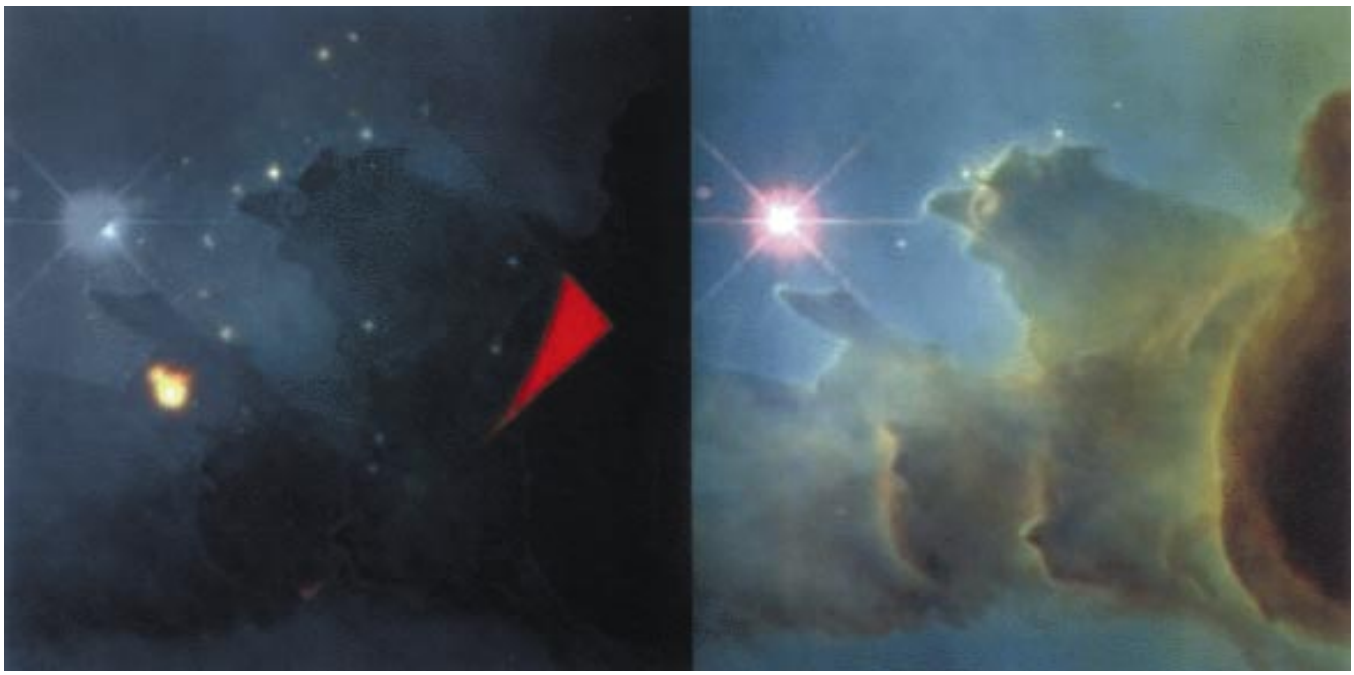

Figure 4: ADONIS observation of Region 367. North is to the bottom left. This picture is rotated by ~90° counterclockwise when compared to Figs. 2 and 3.This region near Walker Star #367 is the primary target region of interest for our M16 observations at La Silla (left). The images in the colour composite consist of the red for K, green for J, and blue for H band observations. The white background image (the "ghost" image) is the Hα data from our WFPC2 observations. This region has a large number of bumps where the photo-erosion process is slowed by positive density fluctuations of different sizes. These specific areas are discussed later. The ADONIS image is 37″ by 37″ which represents four pointings of the 25.6 × 25.6 arcsecond FoV of the SHARP II Camera. The resolution (before image deconvolution) is about 280 mas FWHM for the K-band. This is within a factor of two of that which can be achieved in the visible on the Hubble Space Telescope. The red region at the edge of the left image is the annular mount which holds the beam-splitter, the red colour illustrates the low (300 K) temperature of the emission of this room-temperature object. The high-resolution information obtained by the dual use of Hubble and ADONIS allows a unique probe into the star-forming region. Multiple systems are now resolved.

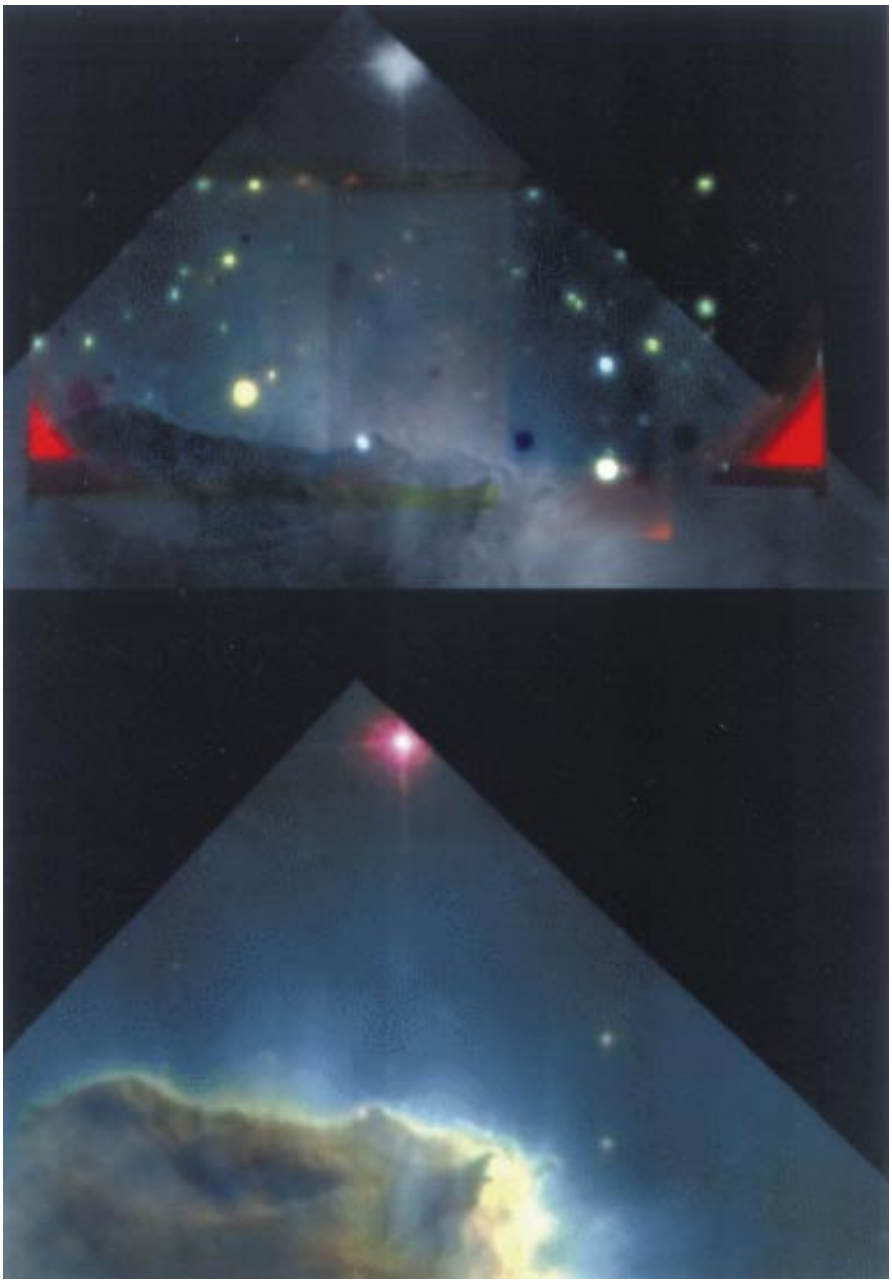

Figure 5: ADONIS observations of TIP (top). North is up. This figure illustrates the region around the "TIP" of Column III. As in Figure 4, this figure is composed of both WFPC2 and ADONIS observations. The region contains a number of protrusions of different sizes and very high activity due to the proximity to the blue stars.
Many of the objects detected in the ADONIS are above and outside of the molecular cloud of the tip, indicating that they are not directly associated with the column.
The outline of this image is 60″ by 32″ which consists of the data from six individual pointings in K band and four pointings in H band and J band. The resolution is about 280 mas (FWHM). This image has the same colour combinations as described for Figure 4.

(3) Investigation of the Very Red Source 367 B

About 10″ from Walker Star 367, there is a very strong infrared source which does not appear in our V filter data. This appears to be a double star which is buried within the column. This may be a star imbedded indeed within the column. Its colours, and the measures of extinction will reveal much about the star, and the internal structure of the column.

Because far-infrared data are needed in order to distinguish the early stage of the individual star-formation regions, the programme at the University of Maryland is currently using data which we have obtained using Hubble WFPC2 data, 350-micron data from Caltech Submillimeter Observatory using the GSFC bolometer array, and the millimetre interferometric observations obtained with the Berkeley-Illinois-Maryland (BIMA) array in addition to the data from the ADONIS observations at ESO.

Figure 2 illustrates the regions observed at La Silla in the context of our recent WPFC2 observations, and Figure 3 shows the context with respect to the existing near infrared observations.

Figures 4 and 5 show the WFPC2 observations at the bottom and the ESO data at the top. At present, the ESO data, with its infrared sensitivity, show far more objects than are visible in the Hubble data.

It is critical to obtain the best resolution in order to understand the extended nature of the objects. To this end, we are using the Lucy algorithm for the deconvolution. This can remove the extended, one-arcsecond skirt of the Adaptive Optics PSF due to the correction residuals, as illustrated in Figure 6. The presence in adaptive optics corrected images of an extended halo around the central high-resolution object is typical. This has been observed and its cause is well understood. It is due to uncorrected higher spatial frequencies, and in some cases to deformable mirror "actuator print-through", whose regular pattern makes four secondary peaks in the PSF. Astronomers who are looking for faint structures underneath this skirt, will have to familiarise themselves with deconvolution, as well as take care that enough SNR is present in the observed object and structure.

A major objective in our high-resolution observations using the ADONIS system has been to identify the relation between the morphology seen in our images from the Hubble Space Telescope and the conventional knowledge concerning the process of star formation as known through observations in the infrared wavelength region. Historically, as shown in the process of obtaining successively higher resolution observations of NGC 6611 (e.g. the successive works of Walker, Chini, and Hillenbrand), the understanding of the physics depends sharply upon the ability to resolve fine features and separate multiple star systems. We now present some of the preliminary results in addressing this relationship. In particular, in this section, we will address three specific features indicated by the morphology of our Hubble Space Telescope images.

The "stalk" star (also known as EGG 041, Hester et. al., 1996) which is indicated as "C" in Figure 7 suggests a density concentration which is resistant to the photo-erosion process, resulting in a sharp protrusion. This is seen as a point source in the visible and a strong, co-located point source in the J, H, and K band. Thus this object appears to be a YSO. However other morphologically interesting features have not, in general, displayed an infrared component. The feature "A" (also known as EGG 039), for example, appears to be a strong density fluctuation with a relatively small characteristic size of a few hundred AU. There is an infrared source (B) which is located relatively

close to A and which has, in the past, been tentatively identified with A. However, the ADONIS data, with their high resolution and suitability for precise astrometry, indicate that this source is most probably a background source. The morphological feature, A, is located approximately 1 arcsecond from the infrared source, B, but is not aligned with the latter. It is unlikely that the infrared source is the uncovered generator of the density fluctuation. Thus it appears that B is a background source and that we do not have, at our current limiting magnitude, a source which appears to be contained in the morphology feature A.

The other area of interest lies above the tip of the large column (Fig. 8). At the top of the column, there are many "fingers" i.e. features which have an extent of approximately 1000 AU in cross dimension and several thousand AU in length. They are then followed by a stem which is bent by approximately 90° and is typically a few thousand AU in extent and attached to the body of the column. These "fingers" are not associated with K-band sources, at our current limiting magnitude. However, one of these objects indicated by "C" in Figure 8 (also known as EGG 001), has been of particular interest. This appears to be an older or more eroded finger. It shows the typical finger structure of Sulphur II emission on the boundary. This eroded finger has two infrared sources, A and B which are located in the vicinity of C. The fainter source B is located more than an arcsecond from the morphology feature. It is also not "in line", so it cannot be the exposed source of the density enhancement which has been "excavated". Source A is located within the morphology feature. However it is located at the trailing end of the finger (with respect to the eroding source) and is significantly asymmetrical with respect to the central axis of C. Thus it likewise does not appear to be associated with C. Most likely, both infrared sources are background objects. The final determination of the status of these objects will result from detailed colour studies of comparing A and B with nearby sources and, perhaps, an evaluation of the silicate absorption feature.

Preliminary Conclusions

The primary scientific conclusions which can be addressed at this time are: (1) the columns appear to be extremely dense (greater than 20 magnitudes of visual extinction over a major part of their area), and (2) the density enhancements identified by the HST images do not contain protostars with a 2-micron signature (at our current level of sensitivity). Most of the stars (seen in the regions which are not obscured by the columns) are background stars in the gal-

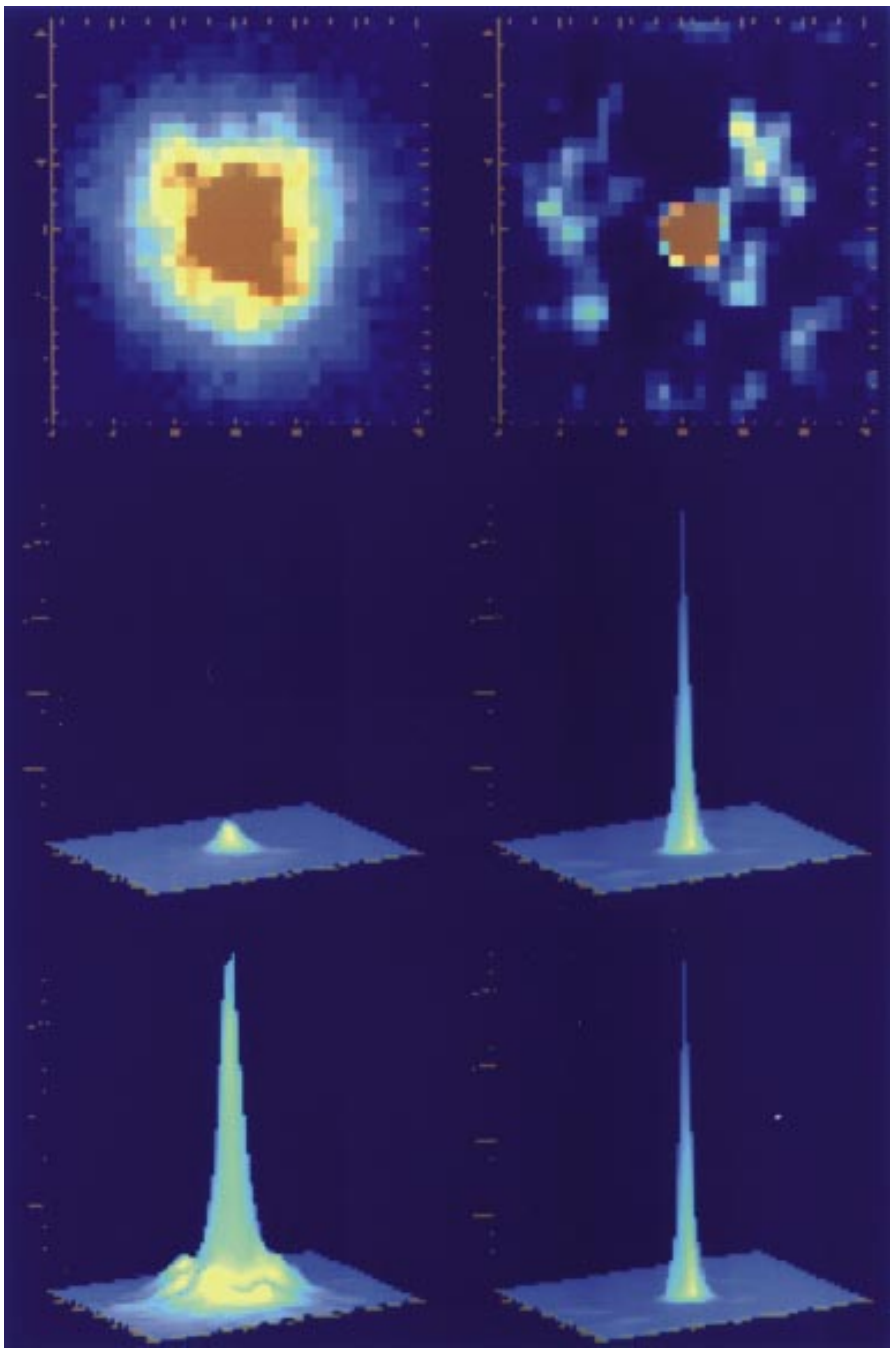

Figure 6: Image Deconvolution in K band: In order to utilise fully the higher frequency components available in the ADONIS data, we need to perform an image deconvolution and/or image reconstruction. For the present data, we use our Lucy-Richardson procedures developed for the Hubble Space Telescope modified for adaptive optics images (Currie et al., 1995). This will allow an improved understanding and identification of the extended and double sources. The top left figure is the image of a (nominally) point source in our K band data set, 27″ from the WFS reference star. The reference star has $m_V = 11.26$ and $B–V = 0.45$. The small patch is 3″ square, and the FWHM of the image from ADONIS is 0.28″ at this offset distance. Due to field anisoplanatism, we see indeed a lowering of the PSF Strehl Ratio to about 8%. This same image is shown in a three-dimensional surface representation in the centre-left and lower left images. The deconvolved images are shown along the right side. In this case, the FWHM of the deconvolved image is 0.13″. The centre image pair is normalised to illustrate the improvement obtained in the Strehl ratio (about a factor of 12, one third of the gain coming from the reduction of the width of the core and the remainder coming from the redistribution of the energy in the extended base of the image) The bottom image pair is normalised to illustrate the narrowing of the peak and the extended structure at the base of the ADONIS image. The wings out to about 1″ are normal for an adaptive optics system. One sees that there are specific features associated with the ADONIS class of AO system. The sub-peaks are probably due to print-through from the regular pattern of actuators in the deformable mirror. This same feature can be seen in the Starfire Optical Range (NM) data described in a earlier publications (Christou et al., 1995 ; Currie et al., 1995). To date we have performed a spatially independent deconvolution but later expect to evaluate the spatially dependent effects and then use our full algorithm.

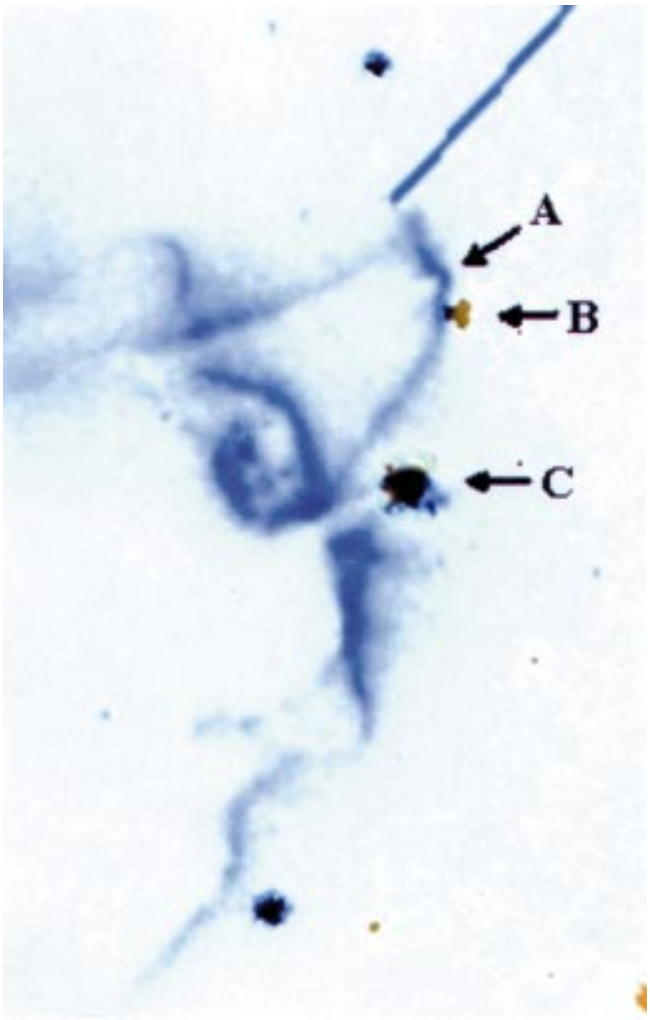

Figure 7: This image is a superposition of the K-band picture obtained using the SHARP II Camera and the ADONIS system on the 3.6-metre telescope at ESO (in red) with the HST image, obtained in the SuI-phur II emission using the F673N filter, displayed in blue. North is up. It is an enlargement of the upper right square inset of Figure 2 near Walker 367. The spatial registration of the two images was obtained by aligning about 15 stars (mostly outside this field of view). The agreement in the positions of these 15 alignment stars is of the order 0.1 arcsecond, over the entire ESO field of view, covering 35 by 35 arcseconds. This internal agreement among the reference stars is more accurate, by a factor of at least 5 times, than the location offsets which are discussed in the text.

106, no. 5, p. 1906–1946, 1993.

4. Walker, H. J. and Wolstencroft, R.D. Cool Circumstellar Matter around Nearby Main-Sequence Stars. *The Astronomical Society of the Pacific*, vol. **100**, p. 1509–1521, 1988.
5. Hester, J. Jeff, Scowen, Paul A., Sankrit, Ravi, Lauer, Tod R., Ajhar, Edward A., Baum, William A., Code, Arthur, Currie, Douglas G., Danielson, G. Edward, Ewald, Shawn P., Faber, Sandra M., Grillmair, Carl J., Groth, Edward J., Holtzman, Jon A., Hunter, Deidre A., Kristian, Jerome, Light, Robert M., Lynds, C. Roger, Monet, David G., O'Neil, Earl J. Jr., Shaya, Edward J., Seidelmann, Kenneth P. and Wesphal, James A. "Hubble Space Telescope WFPC2 Imaging of M16: Photo-evaporation and Emerging Young Stellar Objects." *The Astronomical Journal*, Volume **111**, No. 6, 1996.
6. Currie, Douglas G., Avizonis, Petras V., Dowling, Daniel M., Kissell, Kenneth E., O'Leary, Dianne P., Nagy, James G., and Fugate, Robert Q. "Approaches for Image Processing Supporting Adaptive Optics". 1996. In Proceedings (edited by M. Cullum), Topical Meeting on Adaptive Optics, October 2–6, 1995, Garching bei München, Germany, by the European Southern Observatory, p. 299–304.
7. Christou, J.C., Ellerbroek, B., Fugate, B.Q., Bonaccini, D. and Stanga, R. "Rayleigh Beacon Adaptive Optics Imaging of ADS 9731: Measurements of the Isoplanatic Field of View" , 1995, *ApJ*, **450**, 369–379.

Domenico Bonaccini,
dbonacci@eso.

axy, with significant extinction. From an Adaptive-Optics technology point of view, we have illustrated the potential for a large improvement in the PSF (or Strehl ratio) across the observed field from the use of deconvolution procedures.

It is clear that deconvolution techniques will contribute considerably to the astrophysical throughput of Adaptive Optics. Iterative deconvolution capabilities are being added to the ESO eclipse pipeline processing software, to be used routinely on Adonis data.

References

1. André, P. Low-Mass Protostars and Protostellar Stages. *Astrophysics and Space Science*, vol. **24**, p. 29, 1995.
2. Chini, R. and Wargau, W.F. Abnormal Extinction and Pre-Main Sequence Stars in M16. *Astronomy and Astrophysics*, vol. **227**, p. 213, 1990.
3. Hillenbrand, Lynne A., Massey, Philip, Strom, Stephen E. and Merrill, K. Michael. NGC 6611: A Cluster Caught in the Act. *The Astronomical Journal*, vol.

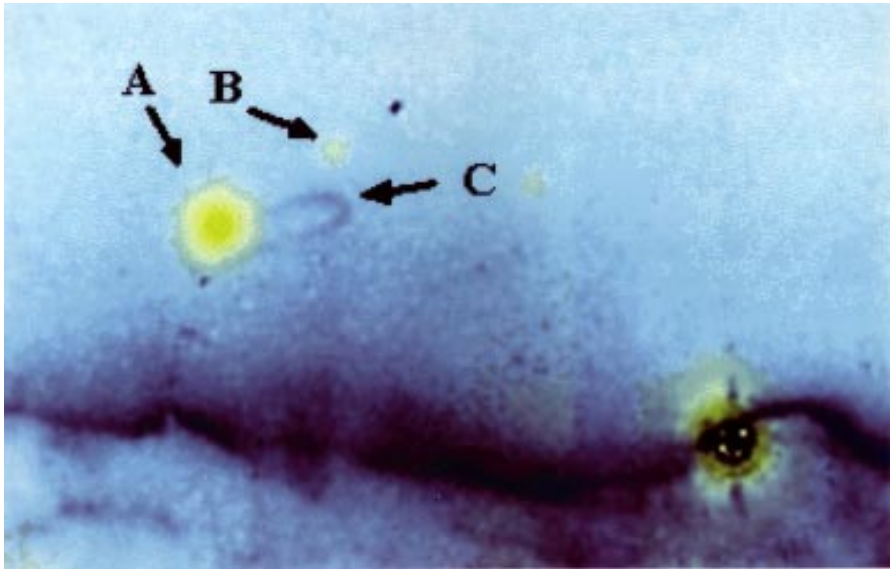

Figure 8: This is a magnified region located above the tip of the largest column in our HST image (see Figs. 2 and 5 – top). North is up. The picture is a superposition of Sharp II K-band and HST images, with the red and blue components as indicated in Figure 7. The astrometric alignment was performed using our centroiding algorithms in order to translate, rotate and rescale the images, as in the above figure. Once again, the agreement in the positions of the 7 reference stars is of the order of 0.1 arcsecond.